

Risk-Aware Human-in-the-Loop Framework with Adaptive Intrusion Response for Autonomous Vehicles

Dawood Wasif¹, Terrence J. Moore², Seunghyun Yoon³, Hyuk Lim³,
Dan Dongseong Kim⁴, Frederica F. Nelson², Jin-Hee Cho¹

¹Virginia Tech, USA ²U.S. Army Research Laboratory, USA

³KENTECH, Republic of Korea ⁴The University of Queensland, Australia

Abstract— Autonomous vehicles must remain safe and effective when encountering rare long-tailed scenarios or cyber–physical intrusions during driving. We present RAIL, a risk-aware human-in-the-loop framework that turns heterogeneous runtime signals into calibrated control adaptations and focused learning. RAIL fuses three cues (curvature actuation integrity, time-to-collision proximity, and observation-shift consistency) into an **Intrusion Risk Score (IRS)** via a weighted Noisy-OR. When IRS exceeds a threshold, actions are blended with a cue-specific shield using a learned authority, while human override remains available; when risk is low, the nominal policy executes. A *contextual bandit* arbitrates among shields based on the cue vector, improving mitigation choices online. RAIL couples Soft Actor–Critic (SAC) with risk-prioritized replay and dual rewards so that takeovers and near misses steer learning while nominal behavior remains covered. On MetaDrive, RAIL achieves a *Test Return (TR)* of 360.65, a *Test Success Rate (TSR)* of 0.85, a *Test Safety Violation (TSV)* of 0.75, and a *Disturbance Rate (DR)* of 0.0027, while logging only 29.07 training safety violations—outperforming RL, safe RL, offline/imitation learning, and prior HITL baselines. Under Controller Area Network (CAN) injection and LiDAR spoofing attacks, it improves *Success Rate (SR)* to 0.68 and 0.80, lowers the *Disengagement Rate under Attack (DRA)* to 0.37 and 0.03, and reduces the *Attack Success Rate (ASR)* to 0.34 and 0.11. In CARLA, RAIL attains a TR of 1609.70 and TSR of 0.41 with only 8K steps.

I. INTRODUCTION

Autonomous vehicles (AVs) are moving from controlled pilots to open-world deployment, promising safer and more efficient transportation by offloading perception, planning, and control from humans to machine intelligence. Progress in large-scale simulation, high-capacity function approximation, and model-based and model-free control has produced competent lane keeping, merging, and urban navigation, often with performance that approaches human driving in benign conditions [1]. As the autonomy stack matures, the community has moved from “can it drive” to “when and why does it fail,” with emphasis on sample efficiency, transfer to unseen maps, and transparent interaction with human operators. This progress raises a central requirement for deployment: AVs must reason about safety and uncertainty while

coordinating seamlessly with human oversight.

The general problem that emerges in safety-critical autonomy is that learned policies are exposed to adversarial perturbations or rare long-tail scenarios that are not fully captured during development. Pure reinforcement learning (RL) can optimize returns in a simulator, yet it may violate safety constraints during exploration. Safe RL methods introduce constraints but often depend on hand-tuned costs and may underperform when the cost signals are sparse or delayed [2], [3]. Imitation learning (IL) jumpstarts behavior but can overfit to the logged distribution and degrade when the environment deviates from training data [4], [5]. Offline RL reduces the risk of data collection but inherits dataset bias and imperfect coverage [6]. Human-in-the-loop (HITL) learning injects expert knowledge through demonstrations, interventions, and shared control [7], yet HITL is largely reactive and fragmented, treating human input as static supervision that does not scale well across diverse environments and attack surfaces. Moreover, in most HITL approaches, when a human takes over, most systems treat the correction as an ad hoc event rather than a structured signal to improve the policy [8], [9], [10].

Significant efforts have attempted to close these gaps. Deep RL baselines such as Soft Actor–Critic (SAC) and Proximal Policy Optimization (PPO) provide data-efficient policy learning for continuous control [11], [12]. Safe RL extends these algorithms with constraint satisfaction and tail-risk objectives [13], [14], [15], [16]. HITL frameworks enable intervention-aware training, copilot optimization, and curriculum shaping [10], [7]. Intrusion detection for vehicular networks and sensors advances the state of the art in anomaly detection and runtime monitoring [17], [18], [19], [20], [21]. Despite substantial progress, practical systems still exhibit important gaps: detection is often decoupled from control, so elevated concern does not translate into calibrated, graded actions at the control rate; human oversight sits outside the primary loop, leaving takeovers and near misses underused as structured supervision; and mitigation logic is largely static, relying on fixed responses rather than adapting with experience in the operator’s domain.

This paper introduces Risk-Aware Human-in-the-Loop with Adaptive Intrusion Response (RAIL), a unified

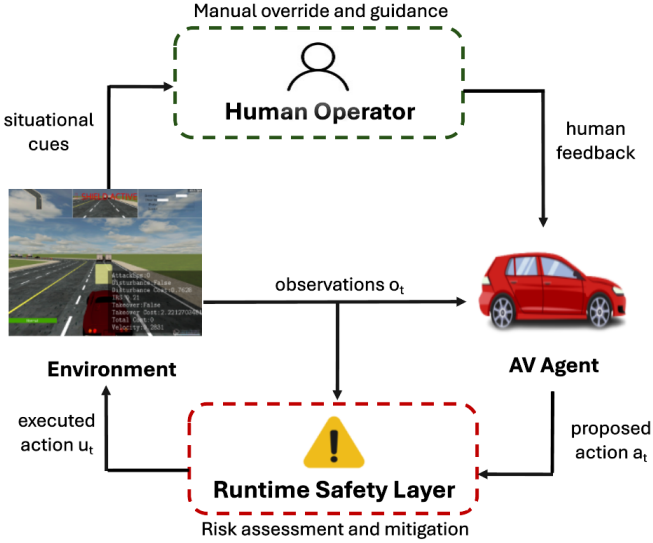


Fig. 1: Paradigm of Risk-Aware HITL Learning

framework for autonomous vehicles that integrates intrusion response and learning into runtime decision making. RAIL couples the control policy with a probabilistic measure of operational concern and converts that concern into interpretable, cue-specific control adjustments blended with the nominal action. A lightweight contextual arbitration mechanism selects which adjustment to apply when concern is high and tunes its strength online based on a success signal correlated with reduced human burden. The learning loop treats human takeovers and safety events as explicit penalties while adding a shaping term that promotes low-concern behavior even before failures occur. A prioritized replay buffer concentrates gradient steps on the most safety-critical slices of experience. Together, these components create a closed loop where detection informs control immediately, choices remain interpretable, and experience continuously improves both the policy and the response mechanism.

Fig. 1 illustrates the high-level paradigm for risk-aware human-in-the-loop learning. The AV agent proposes an action that is first assessed by a runtime safety layer, which mitigates risk before execution. The environment then returns observations, and a human operator can provide situational cues, manual overrides, and feedback. This closed loop ensures that elevated risk is translated into calibrated responses rather than unsafe actuation.

We summarize our **key contributions** as follows:

- We present the Risk-Aware Human-in-the-Loop (RAIL) framework, a unified runtime architecture that links detection, graded response, and human escalation in a single decision loop operating at control rate and logging outcomes for learning.
- We introduce the Intrusion Risk Score (IRS), a probabilistic measure that fuses three runtime cues—*curvature uncertainty* (plan–execute mismatch), *time-to-collision* proximity, and *LiDAR observation*

shift (OOD) detection—into a single value, mapping it to cue-specific, transparent control adjustments that operators can audit, with a contextual selection mechanism that tunes adjustment strength based on current signals and delayed success indicators.

- We advance safety-aware learning by coupling explicit penalties for violations and takeovers with an implicit shaping term that promotes low-concern behavior, and by proposing a replay scheme that prioritizes high-concern and takeover transitions while preserving diversity within an off-policy actor-critic backbone.
- We evaluate RAIL extensively in MetaDrive and CARLA, demonstrating improved safety, robustness, and operator efficiency over RL, safe RL, imitation, offline RL, and prior human-in-the-loop baselines, under both nominal conditions and representative cyber-physical disturbances.

II. RELATED WORK

A. Human-in-the-Loop (HITL) Learning Methods

HITL learning integrates human demonstrations, oversight, and intervention with data-driven control to stabilize training and improve safety in sequential decision-making. In autonomous driving, HITL sits alongside modern deep reinforcement learning approaches such as SAC and PPO that provide strong baselines for continuous control [11], [12], and it complements safe RL methods that enforce constraints during optimization, including constrained policy optimization and PID Lagrangian techniques [2], [3]. Supervised and adversarial imitation methods supply initial competencies from logs, from classical behavioral cloning to distribution-matching via generative adversarial imitation learning [4], [5], while interactive variants collect corrective labels online through expert-in-the-loop aggregation and teleoperation [8], [22]. When direct online exploration is costly or risky, offline RL methods like conservative Q-learning exploit static datasets [6], and recent work demonstrates learning with minimal human effort in real systems as well as shared-autonomy copilot optimization in driving [7], [10], [23]. Despite this progress, many HITL pipelines remain fragmented across learning, safety, and oversight channels, with limited mechanisms to integrate diverse signals and act consistently under uncertainty.

B. Risk-Aware Decision Making

Risk-sensitive reinforcement learning methods model the tails of return distributions using coherent risk measures and distributional critics to attenuate catastrophic outcomes [13], [14]. Surveys emphasize that risk-aware policy optimization is critical for safety-critical robotics and that combining model uncertainty with distributional value estimates improves reliability [15]. Algorithmic advances include proximal policy gradients with safety/risk constraints and hybrid critics mixing mean and tail objectives [16]. Complementary lines impose action filters via runtime shielding or barrier certificates

to guarantee constraint satisfaction even under model mismatch [24], [2]. Nevertheless, many approaches optimize abstract risk on task rewards, leaving open how to *operationalize* risk from multi-source cues [25], [26] (e.g., perception anomalies, V2X disagreements) and how to translate elevated risk into interpretable, graded control responses in real time.

C. Intrusion Detection and Response for AVs

Early automotive security studies demonstrated the feasibility of remotely compromising ECUs and in-vehicle networks, motivating intrusion detection on CAN via specification-based rules and learning-based anomaly models [17], [18], [27], [28], [29]. AV-oriented defenses further introduced runtime monitors that cross-check dynamics, actuator consistency, and state estimation to flag control-relevant anomalies during driving [21]. Concurrently, sensor-level attacks (e.g., LiDAR spoofing, camera adversarial patches) have been demonstrated in the lab and field [20], [19], [20]. Recent intrusion *response* proposals advocate real-time containment, graceful degradation, and cross-layer corroboration under attack [30], [31]. Despite progress, most work isolates detection from control, offers limited, pre-defined mitigation actions, or lacks human-aware escalation strategies; unified, interpretable response policies that fuse cyber and physical risk cues and adapt online to operator feedback remain underexplored.

III. PROPOSED APPROACH: RAIL

We introduce **RAIL** (Risk-Aware Human-in-the-Loop with Adaptive Intrusion Response), which turns runtime risk into graded, interpretable control. The policy proposes an action; a safety layer modulates it, and a human can always overrule.

A. System Overview

We model the ego vehicle at time t with state s_t (ego kinematics, local map features, perception) and a continuous action a_t (steering, longitudinal) sampled from a stochastic policy $\pi_\theta(a_t \mid s_t)$. The environment evolves under the applied control u_t via a transition $p(s_{t+1} \mid s_t, u_t, \xi_t)$ with disturbances ξ_t . RAIL augments this loop with an Intrusion Risk Score $\text{IRS}_t \in [0, 1]$ computed from heterogeneous runtime cues. When risk is low, the nominal action executes ($u_t = a_t$). As risk rises, a cue-specific shield produces a safeguarded proposal \tilde{a}_t and the executor blends it with the policy action; a human override remains available. A lightweight contextual bandit selects the shield and adapts its gain from the current cue vector and delayed success signals. Learning is off-policy with SAC: the replay buffer stores the core transition (s_t, u_t, r_t, s_{t+1}) , with annotations $(a_t, \tilde{a}_t, \text{IRS}_t, c_t, i^*, k_t, \text{flags})$ and prioritizes high-risk or human-corrected transitions so updates focus on safety-critical slices. This architecture couples risk perception, interpretable mitigation, and human supervision within a single closed-loop controller.

B. Intrusion Risk Score (IRS)

The IRS serves as a probabilistic aggregator of multiple cyber-physical risk cues, transforming heterogeneous measurements into a single interpretable value. Formally, at each time step t , we define

$$\text{IRS}_t = 1 - \prod_{i=1}^M (1 - w_i r_i(s_t, a_t)), \quad (1)$$

where M is the number of monitored cues, $r_i(s_t, a_t) \in [0, 1]$ denotes the normalized instantaneous risk contribution of cue i , and w_i are learned importance weights constrained by $\sum_{i=1}^M w_i = 1$. For interpretability, we record the dominant cue $i^* = \arg \max_i w_i r_i(s_t, a_t)$, which indicates the cue contributing most to IRS_t at time t . The multiplicative Noisy-OR form models the probability that at least one cue indicates danger, ensuring that a single high-confidence anomaly (e.g., sudden TTC collapse) is sufficient to elevate IRS_t . Unlike additive scoring, this structure avoids risk underestimation by accounting for inter-cue redundancy and non-linear compounding, effectively capturing how multiple weak but consistent signals may collectively escalate overall risk. Thus, the IRS functions as a latent safety index driving both shield activation and human handover logic. The IRS integrates three ($M = 3$) primary cues as follows.

a) Curvature uncertainty cue: This cue measures control integrity by comparing the planner's intended curvature with the vehicle's executed curvature. The mismatch is converted into a unitless risk in $[0, 1]$, with small tracking errors near zero and sustained bias from faults or injected steering near one.

$$r_{\text{CURV}}(s_t, a_t) = \sigma\left(\frac{|\kappa_{\text{plan}}(s_t) - \kappa_{\text{exec}}(s_t, a_t)|}{\kappa_{\text{max}}}\right). \quad (2)$$

Here s_t is the state, $a_t = [a_t^{\text{steer}}, a_t^{\text{acc}}]$, κ_{plan} is the planned path curvature from route geometry, κ_{exec} is the realized curvature from yaw rate over speed with a small numerical floor, κ_{max} normalizes by feasible limits, and σ is a logistic squashing. Risk grows as the executed path diverges from the intended trajectory.

b) Time-to-collision cue: This cue serves as a physical proximity check, measuring the imminence of hazard by converting available reaction time into risk. Fabricated obstacles or weakened braking shorten the window and increase risk.

$$r_{\text{TTC}}(s_t, a_t) = \exp\left(-\frac{d_t}{\tau_{\text{TTC}} \cdot \max(v_t, \epsilon)}\right), \quad (3)$$

where d_t is the path-aligned distance from the ego bumper to the most threatening object, v_t is the closing speed along the path, $\epsilon > 0$ avoids division by zero when the gap is opening, and τ_{TTC} sets the time scale. The score is near one when contact is imminent and decays smoothly as the available time increases.

Adversarial Driving Context (Sensors + V2X + Environment)

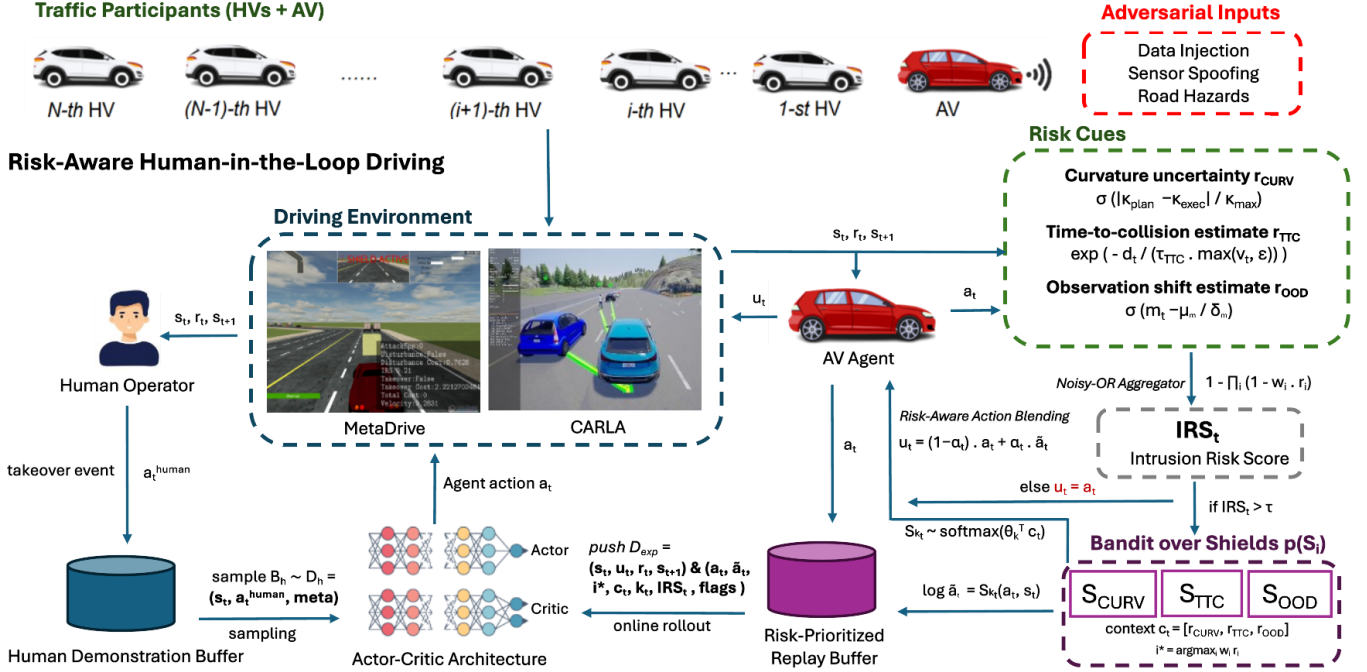


Fig. 2: RAIL System Overview

c) Observation shift cue: This cue detects sensor-level distribution shift in LiDAR returns and is designed to flag spoofing, masking, or blinding that alters the beam pattern beyond nominal variability.

$$r_{OOD}(s_t) = \sigma \left(\frac{\sqrt{(z_t - \mu)^\top (\Sigma + \epsilon I)^{-1} (z_t - \mu)} - \mu_m}{\delta_m} \right), \quad (4)$$

where $z_t \in \mathbb{R}^{72}$ is the LiDAR range vector, (μ, Σ) are the clean-data mean and covariance with Tikhonov regularization ϵI , and (μ_m, δ_m) center and scale the Mahalanobis distance-based score. The risk increases as the current observation becomes less likely under the nominal sensor model.

C. Risk-Aware Action Blending

RAIL turns the policy's proposal into executed control by blending it with a cue-specific safety transform only when runtime risk is elevated. Let a_t be the nominal action and $\tilde{a}_t = S_{k_t}(a_t, s_t)$ the output of shield k_t selected online (e.g., steering guard, brake bias, speed cap), where s_t is the current state. The executor interpolates with authority $\alpha_t \in [0, 1]$ so small risk leaves the policy untouched, while high risk smoothly hands authority to the shield. An exponential moving average smooths the IRS before computing α_t , and a rate limiter bounds changes across cycles.

$$u_t = (1 - \alpha_t) a_t + \alpha_t \tilde{a}_t. \quad (5)$$

The shield selection process is cast as a *contextual bandit* over a small library of interpretable trans-

forms. The context is the current cue vector $c_t = [r_{CURV}, r_{TTC}, r_{OOD}]$. Each arm k carries a linear score $z_{k,t} = \theta_k^\top c_t$ that encodes where that shield is most effective. We sample the arm with a softmax to retain exploration near decision boundaries and to prevent chattering; temperature is annealed over training for convergence.

$$p_t(k) = \frac{\exp(\theta_k^\top c_t)}{\sum_j \exp(\theta_j^\top c_t)}. \quad (6)$$

After executing u_t , a delayed scalar feedback marks success (1 if no takeover within a horizon Δ) and subtracts a small effort penalty $\propto \|\tilde{a}_t - a_t\|$. A lightweight online update nudges θ_{k_t} in the direction of c_t proportional to this feedback, leaving other arms unchanged; this keeps credit assignment local and preserves interpretability. The design yields (i) *locality*—only the risky channel is modified, (ii) *monotonicity*—shield authority grows with risk, and (iii) *auditability*—the active shield, a_t , and scores $\{z_{k,t}\}$ are logged at every step.

D. Risk-Prioritized Replay and Training Procedure

RAIL concentrates learning on safety-critical experience by prioritizing risky or corrected transitions in replay. Each transition stores the core tuple (s_t, u_t, r_t, s_{t+1}) and attaches annotations $(a_t, \tilde{a}_t, IRS_t, c_t, i^*, k_t, \text{flags})$. A scalar priority combines critic TD error (learning progress), intrusion magnitude IRS_t (near misses), and a human-takeover flag (corrective supervision). Sampling is proportional to a powered priority, so batches remain

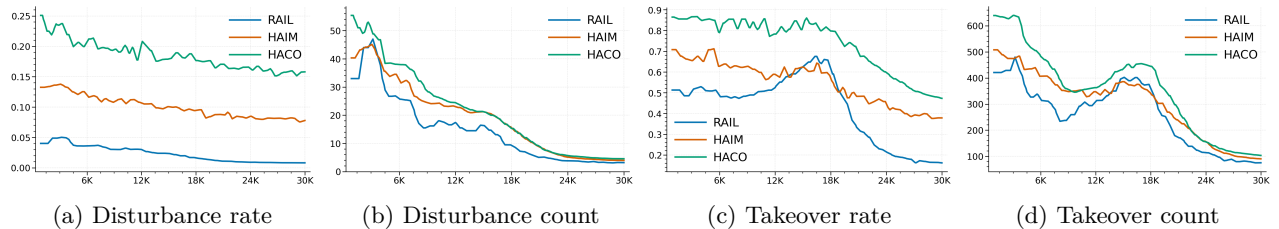


Fig. 3: Training Performance Comparison of RAIL, HAIM [7], and HACO [10] on MetaDrive

diverse while emphasizing consequential events, and per-sample importance weights debias updates. Rollouts always run with risk-aware blending and contextual arbitration; even low-risk steps are retained with small priority to preserve nominal coverage. When $\text{IRS}_t > \tau$, the log additionally records the active shield k_t , the instantaneous authority value α_t inside flags, and a short-horizon outcome tag (no-takeover vs. takeover). Training alternates brief interaction bursts to refresh bandit context with off-policy SAC updates from the prioritized buffer; in practice, human-takeover steps receive the highest priority, followed by high- IRS_t near misses, which accelerates safety alignment and reduces future interventions.

Fig. 2 presents the RAIL system architecture. From state s_t , the policy π_θ proposes a nominal action a_t , which is assessed by three runtime risk cues—curvature uncertainty r_{CURV} , time-to-collision r_{TTC} , and observation shift r_{OOD} —fused into the Intrusion Risk Score (IRS). When IRS exceeds a threshold, a contextual bandit selects a cue-specific shield S_k , and the final control u_t is computed by blending a_t with shield output \tilde{a}_t . Human overrides are possible at any time, and all transitions, annotations, and IRS values are logged into a risk-prioritized replay buffer to guide SAC learning.

IV. EXPERIMENTS AND RESULTS

We design our study around three guiding questions:

- Q1:** *How does RAIL compare to RL, safe RL, offline RL, IL, and HITL baselines in simulation across safety, performance, and traffic friendliness?*
- Q2:** *How robust is RAIL to canonical cyber-physical intrusions relative to strong baselines?*
- Q3:** *Which components of RAIL are most critical to its overall effectiveness?*

A. Experimental Setup

a) Environment & Scenarios: We evaluate in METADRIVE with procedurally generated road graphs (straight segments, curves, T/X intersections, ramps, roundabouts, forks) populated by heterogeneous traffic from stochastic flows. Background vehicles follow IDM longitudinal dynamics and MOBIL lane changing; static cones/barriers and occasional slow movers induce long-tail interactions. Episodes end on goal, collision, off-road,

or timeout (1,000 steps). For cross-simulator generalization, we also test in CARLA with a top-down semantic raster input and identical control heads.

b) Threat Models: *Cyber attack: action-channel injection.* An adversary injects bounded deltas on steering and longitudinal acceleration after the policy but before the safety layer, modeled as $u_t = \text{sat}(a_t + \eta_t)$. Piecewise-constant biases up to 50% full-scale affect either channel for 5 s every 30 s (random start, sign, and channel), emulating ECU/CAN faults that cause unintended steering or throttle/brake bias and testing RAIL’s ability to contain lane departures and near misses. *Physical attack: LiDAR spoofing.* A phantom obstacle is created by overwriting a contiguous azimuth sector in the 72-beam LiDAR with short ranges for a rigid object 4 m ahead, with ± 0.5 m lateral jitter. Bursts last 5 s and recur every 30 s. The spoof feeds the environment’s association, so TTC estimation perceives a plausible target. An attack is deemed successful if a collision or off-road occurs within 3 s after a burst.

c) Baselines: We benchmark RAIL against representative methods spanning RL, safe RL, offline RL and IL, and HITL control. *RL with reward shaping* includes SAC-RS [11] and PPO-RS [12], where “RS” denotes dense penalties on collisions, off-road, and excessive actuation added to the task reward. *Safe RL with explicit cost constraints* comprises SAC-Lag [23] and PPO-Lag [3], which optimize a Lagrangian relaxation with a learned multiplier on episodic cost, and CPO [2], which enforces a trust-region update using a safety critic to satisfy a cost budget. *Offline and imitation learning* baselines are CQL [6], which regularizes Q-values toward conservatism on a fixed dataset, Behavior Cloning (BC) [4] that performs supervised learning on expert state-action pairs, and GAIL [5] that matches expert occupancy via adversarial training. *Conventional HITL* methods include HG-Dagger [8], an interactive aggregation of human corrections into the training buffer, and IWR [22], which upweights human takeover samples through intervention-weighted regression. We further compare to *Human-AI copilot* HACO [10], which blends online human guidance with policy optimization, and *Human as AI Mentor* HAIM-DRL [7], which treats the expert as an online mentor providing corrective signals during exploration. All baselines use the same observation encoder, action bounds, control rate, seeds,

and training budget as RAIL, with algorithm-specific defaults preserved where required by the original papers.

Fig. 3 shows training curves on MetaDrive comparing RAIL with HAIM and HACO. RAIL consistently lowers disturbance and operator takeovers faster than baselines, reaching the lowest steady-state levels across all metrics.

d) Metrics: We evaluate performance and robustness using formally defined, episode-aggregated metrics:

- **Test Success Rate (TSR):** fraction of episodes reaching the goal without collisions or off-road events.
- **Test Return (TR):** expected cumulative reward, reflecting task efficiency.
- **Test Safety Violations (TSV):** number of collisions or lane departures per episode.
- **Disturbance Rate (DR):** fraction of control ticks where acceleration exceeds a comfort bound.
- **Training Safety Violations (TSV_{train}):** cumulative number of safety events during training.
- **Training Data Usage (TDU):** total number of interaction steps during training.
- **Disengagement Rate under Attack (DRA):** fraction of attacked episodes with human takeover.
- **Attack Success Rate (ASR):** fraction of attacked episodes ending in collision or off-road.

e) Implementation details: All methods use SAC with shared hyperparameters (selected through careful tuning using grid search): actor, critic, and entropy learning rates of 1×10^{-4} , batch size 1024, horizon 1,000, learning starts at 100 steps, control at 10 Hz, action clipping, and first-order rate limiting. Observations include ego kinematics, 72-beam LiDAR with 60 m range, side detectors, lane features, and diagnostics used by RAIL. Actions $a_t = [a_t^{\text{steer}}, a_t^{\text{acc}}]$ lie in $[-1, 1]^2$ and map to ± 0.35 rad steering and $[-4.0, 2.5]$ m s⁻². The Intrusion Risk Score uses weights (0.3, 0.4, 0.3) with threshold $\tau = 0.3$. When the score exceeds τ , a contextual selector chooses a shield and the executor blends with authority α_t in [0, 1]. Each method is trained with five random seeds up to a fixed budget of environment interactions or until a validation return plateau, and we keep the best checkpoint on the validation split.

B. Performance Comparison with Baselines

Table I compares reward-shaped RL, safe RL, offline RL, imitation learning (IL), and HITL methods. Reward-shaped RL attains a high return but weaker safety: SAC-RS reaches 384.56 return with 0.87 test safety violations and 0.015 disturbance, while PPO-RS drops to 305.41 return with 4.12 violations and 0.021 disturbance. Safe RL reduces violations relative to PPO-RS but also lowers return and success rate; for instance, SAC-Lag achieves 352.46 return with 0.78 violations and 0.019 disturbance, whereas PPO-Lag yields 298.98 return with 3.28 violations and 0.025 disturbance. Offline and imitation learning baselines perform poorly in this setting: CQL obtains 116.45 return with 3.68 violations and 0.007 disturbance, BC yields 36.13 return with 1.05 violations

and 0.012 disturbance, and GAIL reaches 108.36 return with 4.18 violations and 0.001 disturbance. HITL methods close the gap: HACO achieves 350.01 return with 0.78 violations and 0.038 disturbance, while HAIM-DRL attains 354.34 return with 0.76 violations and 0.0023 disturbance.

RAIL delivers a favorable balance of safety and efficiency with only 30K interaction steps. It achieves 360.65 return and matches the top success rate at 0.85, while reducing test safety violations to 0.75 and keeping disturbance at 0.0027. Training safety violations are also low at 29.07, indicating safer data collection. Compared to HAIM-DRL, RAIL improves return, maintains comparable disturbance and success, and substantially outperforms reward-shaped PPO and SAC on safety. These results show that RAIL preserves HITL sample efficiency, improves safety without sacrificing task performance, and narrows the gap to expert-level stability. A similar trend holds in CARLA, where RAIL attains 1609.70 return and 0.41 success rate with only 8K samples (Table II).

C. Robustness to Intrusions

Table III shows that **RAIL** is the most robust under both intrusion settings. Under CAN injection, RAIL attains the highest test success rate (TSR 0.68) versus PPO 0.23, HACO 0.58, and HAIM 0.62. It also cuts disengagements (DRA 0.37) far below HACO 0.90 and HAIM 0.74, while almost halving attack success (ASR 0.34 vs. HAIM 0.65 and PPO 0.62). Under LiDAR spoofing, RAIL again leads with SR 0.80, achieves near-zero DRA 0.03 compared to HAIM 0.17 and HACO 0.24, and reduces ASR to 0.11 from HAIM 0.20 and HACO 0.29. These outcomes indicate that RAIL’s cue-driven shielding contains actuation corruption and phantom obstacles without collapsing into conservative behavior or relying on frequent human takeover. The simultaneous gains in SR and reductions in DRA and ASR suggest effective containment rather than avoidance, lowering operator burden while preserving task performance in contested conditions.

D. Ablation Study of RAIL Components

Table IV indicates that **TTC** is the most critical cue: removing it degrades SR to 0.67 and sharply increases both SV (1.02) and DR (0.022), confirming its role in imminent-collision mitigation. The **curvature** cue is next in importance (SR 0.78, SV 0.80, DR 0.014), reflecting its contribution to actuation integrity. Dropping the **OOD** cue yields near-normal SR (0.83) but higher DR (0.0049) and slightly worse SV, suggesting reduced caution at higher speeds (AS 23.3). Adaptive **bandit** arbitration matters: fixed shields raise SV (1.10) and DR (0.018) while lowering AS. Uniform IRS weights also hurt DR and AS. Finally, removing the **shield penalty** induces over-use of shielding—SR falls to 0.74 and AS

TABLE I: Performance comparison of RL, safe RL, offline RL, imitation learning (IL), and human-in-the-loop (HITL) methods on MetaDrive. Values are mean \pm standard deviation over five seeds; best results are in **bold**.

Category	Method	Total Training Safety Violation	Training Data Usage	Test Return	Test Safety Violation	Disturbance Rate	Test Success Rate
<i>Expert</i>	Human	–	–	388.16 \pm 45.00	0.03 \pm 0.00	0	1.00
RL	SAC-RS [11]	2.78K \pm 0.97K	1M	384.56 \pm 37.5	0.87 \pm 1.47	0.015 \pm 0.005	0.83 \pm 0.32
	PPO-RS [12]	27.51K \pm 3.86K	1M	305.41 \pm 14.23	4.12 \pm 1.24	0.021 \pm 0.014	0.67 \pm 0.12
Safe RL	SAC-Lag [23]	1.98K \pm 0.75K	1M	352.46 \pm 108.78	0.78 \pm 0.58	0.019 \pm 0.007	0.71 \pm 0.79
	PPO-Lag [3]	15.46K \pm 5.13K	1M	298.98 \pm 50.99	3.28 \pm 0.38	0.025 \pm 0.016	0.52 \pm 0.27
	CPO [2]	4.36K \pm 2.22K	1M	194.06 \pm 108.86	1.71 \pm 1.02	–	0.21 \pm 0.29
Offline RL	CQL [6]	–	49K	116.45 \pm 34.94	3.68 \pm 7.61	0.007 \pm 0.006	0.13 \pm 0.09
IL	BC [4]	–	49K	36.13 \pm 10.06	1.05 \pm 0.54	0.012 \pm 0.017	0.01 \pm 0.02
	GAIL [5]	3.68K \pm 3.17K	49K	108.36 \pm 16.08	4.18 \pm 1.25	0.001 \pm 0.0009	0.03 \pm 0.01
Conventional HITL	HG-Dagger [8]	35.58	50K	106.21	2.63	0.108	0.04
	IWR [22]	69.74	50K	298.87	3.61	0.122	0.61
Human-AI Copilot	HACO [10]	30.05 \pm 10.89	30K	350.01 \pm 9.72	0.78 \pm 0.85	0.038 \pm 0.0083	0.83 \pm 0.07
Human as AI Mentor	HAIM-DRL [7]	29.84 \pm 10.25	30K	354.34 \pm 11.08	0.76 \pm 0.28	0.0023 \pm 0.00072	0.85 \pm 0.03
Risk-Aware HITL	RAIL (Ours)	29.07 \pm 11.36	30K	360.65 \pm 23.06	0.75 \pm 0.03	0.0027 \pm 0.00052	0.85 \pm 0.07

TABLE II: CARLA simulator generalization.

Method	Training Data	TSV \downarrow	TR \uparrow	TSR \uparrow
PPO [12]	500K	80.84	1591.00	0.35
HACO [10]	8K	12.14	1578.43	0.35
HAIM [7]	8K	11.25	1590.85	0.38
RAIL (Ours)	8K	12.38	1609.70	0.41

(Note: TSV \downarrow =test safety violations; TR=test return; TSR \uparrow =test success rate.)

TABLE III: Robustness on MetaDrive under cyber and physical *intrusion* attacks.

Method	CAN Injection		LiDAR Spoof	
	TSR \uparrow / DRA \downarrow / ASR \downarrow	TSR \uparrow / DRA \downarrow / ASR \downarrow	TSR \uparrow / DRA \downarrow / ASR \downarrow	TSR \uparrow / DRA \downarrow / ASR \downarrow
PPO [12]	0.23 / 0.85 / 0.62	0.49 / 0.21 / 0.23		
HACO [10]	0.58 / 0.90 / 0.75	0.74 / 0.24 / 0.29		
HAIM [7]	0.62 / 0.74 / 0.65	0.77 / 0.17 / 0.20		
RAIL (Ours)	0.68 / 0.37 / 0.34	0.80 / 0.03 / 0.11		

(Note: Each cell reports **TSR** (Test Success Rate), **DRA** (Disengagement Rate under Attack), and **ASR** (Attack Success Rate).)

to 16.6, showing the penalty is needed to prevent overly conservative behavior while maintaining low DR.

Fig. 4 illustrates qualitative examples where IRS spikes trigger dominant cue selection and shielded controls. For each cue (curvature, TTC, OOD), RAIL responds with targeted interventions that avert incidents while maintaining driving progress.

V. CONCLUSIONS & FUTURE WORK

We presented RAIL, a risk-aware human-in-the-loop framework that fuses heterogeneous runtime cues into an Intrusion Risk Score, blends nominal and safeguarded controls via interpretable shields, arbitrates with a contextual bandit, and learns with dual rewards plus risk-

TABLE IV: RAIL ablations on MetaDrive.

Variant	SR \uparrow	SV \downarrow	DR \downarrow	AIRS \downarrow	AS \uparrow
w/o curvature cue	0.78	0.80	0.0140	0.17	22.7
w/o TTC cue	0.67	1.02	0.0220	0.12	22.5
w/o OOD cue	0.83	0.77	0.0049	0.15	23.3
w/o bandit (fixed)	0.79	1.10	0.0180	0.16	19.7
w/o weights (uniform)	0.81	0.79	0.0056	0.16	20.4
w/o shield penalty	0.74	0.72	0.0044	0.12	16.6
RAIL (full)	0.85	0.75	0.0027	0.15	22.8

(Note: SR \uparrow = success rate; SV \downarrow = safety violations; DR \downarrow = disturbance rate; AIRS \downarrow = average Intrusion Risk Score per episode; AS \uparrow = average speed (km/h))

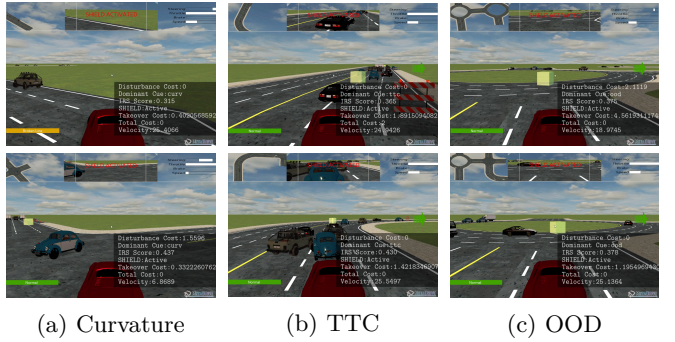


Fig. 4: Qualitative Cue-Driven IRS Responses

prioritized replay. On MetaDrive, RAIL improves safety and robustness over RL, safe RL, imitation, offline RL, and prior HITL baselines, lowering disturbance and disengagement while maintaining competitive success and return. Under cyber and physical intrusions, RAIL lowers attack success and the need for operator handovers, demonstrating that intrusion-aware shaping plus online shield adaptation translates concern into graded control actions, preserving stability and mission progress rather

than triggering an all-or-nothing fail-safe.

For **future work**, we will broaden cue coverage (e.g., richer perception consistency checks), study adaptive thresholds and shield parameterization with formal safety envelopes, and scale to multi-agent traffic with cooperative risk sharing. We also plan to transfer to hardware-in-the-loop tests, expand human factors evaluation of transparency and workload, and integrate stronger attack generation to stress-test generalization.

REFERENCES

- [1] D. Parekh, N. Poddar, A. Rajpurkar, M. Chahal, N. Kumar, G. P. Joshi, and W. Cho, “A review on autonomous vehicles: Progress, methods and challenges,” *Electronics*, vol. 11, no. 14, p. 2162, 2022.
- [2] J. Achiam, D. Held, A. Tamar, and P. Abbeel, “Constrained policy optimization,” in *International conference on machine learning*. PMLR, 2017, pp. 22–31.
- [3] A. Stooke, J. Achiam, and P. Abbeel, “Responsive safety in reinforcement learning by pid lagrangian methods,” in *International Conference on Machine Learning*. PMLR, 2020, pp. 9133–9143.
- [4] M. Bain and C. Sammut, “A framework for behavioural cloning,” in *Machine intelligence* 15, 1995, pp. 103–129.
- [5] J. Ho and S. Ermon, “Generative adversarial imitation learning,” *Advances in neural information processing systems*, vol. 29, 2016.
- [6] A. Kumar, A. Zhou, G. Tucker, and S. Levine, “Conservative q-learning for offline reinforcement learning,” *Advances in neural information processing systems*, vol. 33, pp. 1179–1191, 2020.
- [7] Z. Huang, Z. Sheng, C. Ma, and S. Chen, “Human as ai mentor: Enhanced human-in-the-loop reinforcement learning for safe and efficient autonomous driving,” *Communications in Transportation Research*, vol. 4, p. 100127, 2024.
- [8] M. Kelly, C. Sidrane, K. Driggs-Campbell, and M. J. Kochenderfer, “Hg-dagger: Interactive imitation learning with human experts,” in *2019 International Conference on Robotics and Automation (ICRA)*. IEEE, 2019, pp. 8077–8083.
- [9] W. Saunders, G. Sastry, A. Stuhlmüller, and O. Evans, “Trial without error: Towards safe reinforcement learning via human intervention,” *arXiv preprint arXiv:1707.05173*, 2017.
- [10] Q. Li, Z. Peng, and B. Zhou, “Efficient learning of safe driving policy via human-ai copilot optimization,” *arXiv preprint arXiv:2202.10341*, 2022.
- [11] T. Haarnoja, A. Zhou, P. Abbeel, and S. Levine, “Soft actor-critic: Off-policy maximum entropy deep reinforcement learning with a stochastic actor,” in *International conference on machine learning*. Pmlr, 2018, pp. 1861–1870.
- [12] J. Schulman, F. Wolski, P. Dhariwal, A. Radford, and O. Klimov, “Proximal policy optimization algorithms,” *arXiv preprint arXiv:1707.06347*, 2017.
- [13] A. Tamar, Y. Glassner, and S. Mannor, “Optimizing the cvar via sampling,” in *Proceedings of the AAAI Conference on Artificial Intelligence*, vol. 29, no. 1, 2015.
- [14] I. Greenberg, Y. Chow, M. Ghavamzadeh, and S. Mannor, “Efficient risk-averse reinforcement learning,” *Advances in Neural Information Processing Systems*, vol. 35, pp. 32639–32652, 2022.
- [15] J. Queeney and M. Benosman, “Risk-averse model uncertainty for distributionally robust safe reinforcement learning,” *Advances in Neural Information Processing Systems*, vol. 36, pp. 1659–1680, 2023.
- [16] Z. Yang, H. Jin, Y. Tang, and G. Fan, “Risk-aware constrained reinforcement learning with non-stationary policies,” in *Proceedings of the 23rd International Conference on Autonomous Agents and Multiagent Systems*, 2024, pp. 2029–2037.
- [17] J. Nagarajan, P. Mansourian, M. A. Shahid, A. Jaekel, I. Saini, N. Zhang, and M. Kneppers, “Machine learning based intrusion detection systems for connected autonomous vehicles: A survey,” *Peer-to-Peer Networking and Applications*, vol. 16, no. 5, pp. 2153–2185, 2023.
- [18] K.-T. Cho and K. G. Shin, “Fingerprinting electronic control units for vehicle intrusion detection,” in *25th USENIX security symposium (USENIX Security 16)*, 2016, pp. 911–927.
- [19] H. Ren and T. Huang, “Adversarial example attacks in the physical world,” in *International Conference on Machine Learning for Cyber Security*. Springer, 2020, pp. 572–582.
- [20] F. Aloraini, A. Javed, and O. Rana, “Adversarial attacks on intrusion detection systems in in-vehicle networks of connected and autonomous vehicles,” *Sensors*, vol. 24, no. 12, p. 3848, 2024.
- [21] R. Sultana, J. Grover, M. Tripathi, and P. Sharma, “Ladetects: Local and adaptive data-centric misbehavior detection framework for vehicular technology security,” *IEEE Open Journal of Vehicular Technology*, 2024.
- [22] A. Mandlekar, D. Xu, R. Martín-Martín, Y. Zhu, L. Fei-Fei, and S. Savarese, “Human-in-the-loop imitation learning using remote teleoperation,” *arXiv preprint arXiv:2012.06733*, 2020.
- [23] S. Ha, P. Xu, Z. Tan, S. Levine, and J. Tan, “Learning to walk in the real world with minimal human effort,” *arXiv preprint arXiv:2002.08550*, 2020.
- [24] M. Alshiekh, R. Bloem, R. Ehlers, B. Könighofer, S. Niekum, and U. Topcu, “Safe reinforcement learning via shielding,” in *Proceedings of the AAAI conference on artificial intelligence*, vol. 32, no. 1, 2018.
- [25] I. L. Johansen and M. Rausand, “Foundations and choice of risk metrics,” *Safety science*, vol. 62, pp. 386–399, 2014.
- [26] M. Pendleton, R. Garcia-Lebron, J.-H. Cho, and S. Xu, “A survey on systems security metrics,” *ACM Computing Surveys (CSUR)*, vol. 49, no. 4, pp. 1–35, 2016.
- [27] A. Tamar, Y. Chow, M. Ghavamzadeh, and S. Mannor, “Policy gradient for coherent risk measures,” *Advances in neural information processing systems*, vol. 28, 2015.
- [28] T. Kastner, M. A. Erdogdu, and A.-m. Farahmand, “Distributional model equivalence for risk-sensitive reinforcement learning,” *Advances in Neural Information Processing Systems*, vol. 36, pp. 56 531–56 552, 2023.
- [29] G. Choudhary, V. Sharma, I. You, K. Yim, R. Chen, and J.-H. Cho, “Intrusion detection systems for networked unmanned aerial vehicles: A survey,” in *2018 14th International Wireless Communications & Mobile Computing Conference (IWCMC)*. IEEE, 2018, pp. 560–565.
- [30] M. Hamad, A. Finkenzeller, M. Kühr, A. Roberts, O. Maennel, V. Prevelakis, and S. Steinhorst, “React: Autonomous intrusion response system for intelligent vehicles,” *Computers & Security*, vol. 145, p. 104008, 2024.
- [31] A. Abdo, S. M. B. Malek, X. Zhao, and N. Abu-Ghazaleh, “Avmon: securing autonomous vehicles by learning control invariants and residual prediction,” in *Symposium on Vehicle Security and Privacy (VehicleSec)*, 2024.